Dynamics of a vector spin-glass model

Shang-keng Ma
Department of Physics and Institute for Pure & Applied Physical Sciences, University of California, San Diego, La Jolla, California 92093
(Received 25 March 1980)

We examine a model of spin-$\frac{1}{2}$ vectors randomly distributed and interacting via a $\pm r^{-3}$ law with random signs. Here r is the interspin distance. A mean-field theory is derived from the variational principle. Strongly coupled pairs, trios, and aggregates of more spins appear as more complicated single spins. The concept of local fields, including anisotropy fields emerges naturally. Statistics of local fields and metastable states are estimated. The magnetic susceptibility and the remanent magnetization at low temperatures are studied. Their time dependence and dependence on the applied field are calculated approximately.

I. INTRODUCTION

Spin-glasses which have been studied most extensively in the laboratories are magnetic ions randomly distributed in a host metal. The classic example is a system of Mn ions in Cu. Recent experiments have accumulated a vast amount of data on the low-temperature properties of spin-glasses.[1-3] Among the many interesting phenomena observed are the remanent magnetization (which remains after the external field is turned off) and their extremely slow decay, the slowly varying susceptibility, hysteresis, etc.

Theoretical investigations of these time-dependent phenomena in spin-glasses have been lagging behind the experimental work. Because of the complexity of the system, studies which are most relevant to observations often have been numerical or partially numerical in nature. Monte Carlo simulations with Ising spin-glass by Kinzel and others[4] demonstrated qualitatively remanent magnetizations and other phenomena resembling those observed empirically. More recently Dasgupta, Ma, and Hu[5] showed that, again for an Ising spin-glass model, the low-temperature phenomena observed in Monte Carlo simulations can be adequately explained by the dynamics of small spin clusters in a frozen background. Each cluster by definition has a metastable state and a stable state. The statistics of the barrier heights and energies of the metastable states were obtained numerically and also by analytic approximations. From the statistics, remanents, susceptibility, and other quantities were calculated.

The Ising spin-glass model used in Refs. 4 and 5 is very different from the real spin-glasses in which the spins are quantum-mechanical vectors. Furthermore, the spin-spin interaction in real spin-glasses such as MnCu is the long-range Ruderman-Kittel-Kasuya-Yosida (RKKY) interaction,[6] which is not well represented by the Gaussian-distributed nearest-neighbor interaction of most Ising spin-glass models. Walker and Walstedt[7] have studied a more realistic model with RKKY interaction by numerical simulation. They have determined the ground-state spin configuration and the spin-wave spectrum. They have obtained all major results except dynamic phenomena involving metastable states. Very good agreement with experiments was found.

It is our purpose here to extend the simple physical picture of small clusters of Ref. 5 so as to include the long-range force, and the quantum and vector nature of the spins. This work is exploratory and qualitative. No numerical and quantitative calculations like those in Ref. 5 are attempted here. We study the low-temperature time-dependent properties of a model of randomly distributed spin $\frac{1}{2}$'s. The spin-spin interaction is $-J_{ij}\vec{s}_i\cdot\vec{s}_j$ with

$$J_{ij} \propto \pm 1/|\vec{r}_i - \vec{r}_j|^3 \ , \tag{1.1}$$

where the $\pm$ sign is randomly assigned. This is not quite the RKKY interaction which has an extra cos $2k_F|\vec{r}_i-\vec{r}_j|$ factor with k_F being the Fermi momentum of the host metal electrons.

It turns out that this model is far more involved than the Ising spin-glass model although some of the basic features remain. The analysis of Ref. 5 cannot be generalized easily to study this model. What will be presented in the following sections is a crude analysis based on a generalized mean-field theory, together with plausible arguments and assumptions. A simple qualitative physical picture does emerge and orders of magnitude of various quantities of interests are obtained. We now outline our approach and

 ©1980 The American Physical Society

summarize our results.

The spin-glass at very low temperature is characterized by a frozen random spin configuration. This physical picture is well described by a mean-field approximation. Each spin points along the local field produced by all the other spins. This approximation follows from a simple variational trial wave function for the ground state. The problem of energy minimization is the problem of finding the local fields and spin orientations self-consistently. We do not attempt to solve this self-consistent field problem. Instead we estimate the distribution of the local fields by first assuming the spin orientations of neighbors are random. Then we estimate the correction due to the energy-minimum condition. The correction has the effect of creating a "cavity" centered around $\vec{h}=0$. Figure 1(a) shows schematically the effect of the cavity. At zero temperature the distribution at $h=0$ must vanish. This effect has been observed in many numerical calculations.[7,8]

Next, we modify the variational trial wave function to give a more careful treatment of strongly coupled pairs. Owing to the very wide distribution of coupling strength J_{ij} in this model, there are many pairs with very large J_{ij}. We study the energy of a strongly coupled pair in the mean fields provided by neighbors. There are two mean fields: $\vec{h}$ couples to the total spin of the pair and an "anisotropy field" $\vec{h}^*$, which enters the energy quadratically and has the effect of an anisotropy. The analysis is then extended to strongly coupled trios and in general "nuclei" of any number of strongly coupled spins. The mean fields for a nucleus include two or more anisotropy fields. The energy levels for a nucleus in a given set of mean fields are described by an effective Hamiltonian

$$H_{\text{eff}}=K^*_{\alpha\beta}s_\alpha s_\beta-\vec{h}\cdot\vec{s}\ , \tag{1.2}$$

where $\vec{s}$ is the total spin of the nucleus. The symmetric tensor $K^*_{\alpha\beta}$ is a quadratic function of all the anisotropy fields. It can be called the "anisotropy energy tensor" for the nucleus. The properties of metastable states can be calculated in principle from $K^*_{\alpha\beta}$, $\vec{h}$ together with information concerning the neighbors. The neighbors always readjust as the spin of the nucleus is rotated. A nucleus, together with its surrounding neighbors, plays the role of a "cluster." Metastable states must be described in terms of such clusters, not just the nuclei.

The distributions of the mean fields for nuclei are then estimated by assuming random spin orientations first and then looking for corrections. Figure 1(b) shows the distribution of $\vec{h}$ for a given K^*. Again we see a cavity on a bell shaped curve. This cavity is not as deep as that in Fig. 1(a). As long as K^* is not zero, it is possible to have pairs with $\vec{h}=0$. Metastable states tend to have small h. The cavity grows deeper as more metastable states decay. The change of the cavity under the influence of an external applied field $\vec{h}_A$ tells us about the magnetic susceptibility and the remanent magnetization.

At very low temperatures, (T much less than the spin-glass transition temperature), the susceptibility has a constant part, coming from the fast response to the external field, and a slowly varying part χ^* which comes from the metastable states. Figure 2 shows

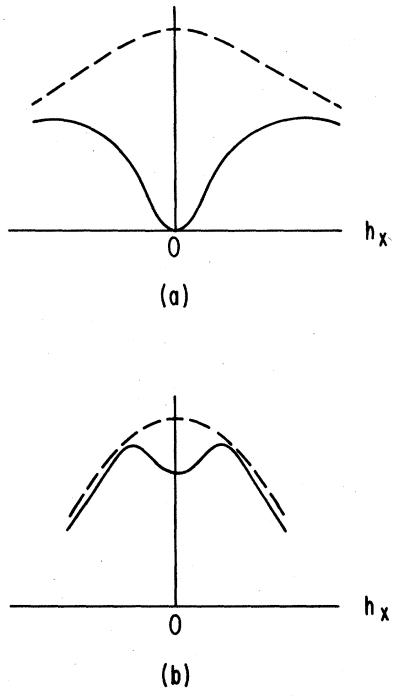

FIG. 1. (a) Schematic plot of the probability distribution of local fields for spins along one axis. The dash curve is estimated from random orientations of neighbors. The solid curve includes the correction due to minimizing the energy. The suppression near $h=0$ creates a "cavity" in the distribution. (b) The local-field distribution of nuclei. The cavity is not as deep as the case for single spins shown in (a) because of the stabilizing effect of anisotropy fields.

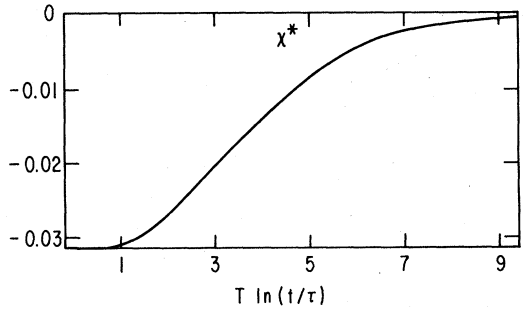

FIG. 2. Time varying part of the magnetic susceptibility per nucleus as a function of $T\ln(t/\tau)$ for small T. (Details in Sec. V.)

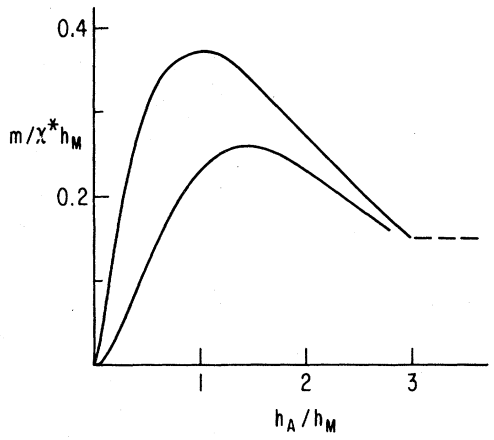

FIG. 3. Remanent magnetizations as functions of the applied field h_A, upper curve TRM, lower curve IRM. (Details in Sec. VI.)

the susceptibility as a function of $T\ln(t/\tau)$. Here τ measures the microscopic transition time due to spin-lattice interaction. The time scale for τ in a real system is about 10^{-10} sec. For $t\sim 1$ sec, $\ln(t/\tau)\sim 23$. Figure 3 shows the remanent magnetization as a function of the applied field h_A which was present. TRM stands for thermal remanent magnetization. The sample was cooled from high temperatures in the field $\vec{h}_A$. Then $\vec{h}_A$ is turned off. IRM stands for isothermal remanent magnetization. The sample was cooled from high temperatures without $\vec{h}_A$. Then $\vec{h}_A$ was turned on and then off. The remanent magnetization peaks at $h_A\approx h_M$. The effect of turning $\vec{h}_A$ on or off is partly to stir up the spins. h_M is the field strength below which the memory of spins survives the stirring. Our crude approximations do not say anything about the "saturation remanent" at large h_A except that it should be smaller than the peak TRM value by a factor $\sim 1/\sqrt{n}$, where $n\sim 10$ is the effective number of neighbors of a nucleus which acts as the center of a cluster.

The mean-field approximation for the spins and nuclei is formulated in Sec. II. Estimates of various distributions are done in Sec. III. We devote Sec. IV to some mathematics involved in calculating the slow time variations due to metastable states. The magnetic susceptibility is calculated in Sec. V, and the remanent magnetization is studied in Sec. VI. Further discussions of the results are included in Sec. VII. The Appendix collects some algebraic details which may be of interest to some readers. It includes the calculation of the local-field distributions from random spins and the derivation of the effective Hamiltonian for a strongly coupled trio.

II. MEAN-FIELD APPROXIMATION

A. The model

We shall consider the spins (quantum spin-$\frac{1}{2}$ operators) $\vec{s}_i$, $i=1,\ldots,N$. The spins are randomly distributed in a volume V. Their Hamiltonian is

$$H=H_0+H_{\rm sl}\ , \tag{2.1}$$

where H_0 is the spin-spin interaction term

$$H_0=-\tfrac{1}{2}\sum_{i/j}J_{ij}\vec{s}_i\cdot\vec{s}_j-\vec{h}_A\cdot\sum_i\vec{s}_i\ ,$$
$$J_{ij}=A\,\tau_{ij}/r_{ij}^3\ ,\quad r_{ij}\equiv|\vec{r}_i-\vec{r}_j|\ , \tag{2.2}$$

and $\vec{h}_A$ is the applied field. Here $\tau_{ij}=\pm 1$ is a randomly chosen sign and $\vec{r}_i$ is the position of the ith spin. A is a constant. Equation (2.2) is to simulate the RKKY interaction, which is more complicated

$$J_{ij}^{\rm RKKY}=A\cos(2k_Fr_{ij})/r_{ij}^3\ . \tag{2.3}$$

This describes the interaction between impurity spins in a metal host. k_F is the Fermi momentum of the conduction electrons. For a derivation and discussion of this formula, see Ref. 6. In Eq. (2.2), we use the random sign τ_{ij} to simulate the $\cos 2k_Fr$ in $J^{\rm RKKY}$.

The term $H_{\rm sl}$ is the "spin-lattice" interaction which describes the effect of the background lattice on the spins. It is assumed to be a weak term. It causes transitions among the energy levels of H_0. We assume the form

$$H_{\rm sl}=\sum_i\vec{s}_i\cdot\vec{L}_i\ , \tag{2.4}$$

where $\vec{L}_i$ are some operators involving the dynamic variables of the lattice. In short, we assume that the allowed transitions under $H_{\rm sl}$ are single-spin-flip transitions. We shall not be interested in more details about $H_{\rm sl}$.

Let us now concentrate on H_0 with $h_A=0$. The scales of length and energy are, respectively, fixed by

$$\tilde{r}\equiv(V/N)^{1/3}\ ,\quad \tilde{J}\equiv s^2A/\tilde{r}^3=NA/4V\ . \tag{2.5}$$

We shall choose $\tilde{r}$ and $\tilde{J}$ as units of length and energy, respectively. As a reference, we note that for 1 at.% Mn in Cu, $s^2A/r^{-3}\sim 20$ K ($s=\frac{5}{2}$ for Mn), which is roughly the observed spin-glass transition temperature.[9] Although we shall not calculate the transition temperature T_c for our model here, we expect $\tilde{J}$ to be of the same order of magnitude of T_c. Thus, in our units, $\tilde{r}=1$, $\tilde{J}=1$, and T_c is about one or two.

B. Variational principle

We shall formulate the basic concepts in terms of the variational principle. We shall not use the variational principle for quantitative calculations, but only use it as a basis for constructing a simple physical picture.

Suppose that we want to find the ground state of the Hamiltonian H_0. We start with the trial wave function

$$\Psi = \prod_{i=1}^{N} \psi_i(\hat{n}_i) \ , \tag{2.6}$$

where $\hat{n}_i$ are unit vectors which are the variational parameters. ψ_i is the wave function for the single spin i, and is such that

$$\langle \psi_i | \vec{s}_i | \psi_i \rangle = \tfrac{1}{2} \hat{n}_i \ . \tag{2.7}$$

The average energy over this trail wave function is simply

$$E_0[\hat{n}] \equiv \langle \Psi | H_0 | \Psi \rangle = -\tfrac{1}{2} \sum_{i,j} J_{ij} \hat{n}_i \cdot \frac{\hat{n}_j}{4}$$

$$= -\tfrac{1}{2} \sum_{i,j} \frac{\tau_{ij}}{r_{ij}^3} \hat{n}_i \cdot \hat{n}_j \tag{2.8}$$

in the units $\tilde{r} = 1$ and $\tilde{J} = 1$ [see Eq. (2.5)]. The variational principle says that E_0 must be stationary under an infinitesimal rotation $\vec{\theta}_i$ of any $\hat{n}_i$, i.e.,

$$-\vec{\theta}_i \times \hat{n}_i \cdot \frac{\partial E}{\partial \hat{n}_i} = \vec{\theta}_i \times \hat{n}_i \cdot \vec{h}_i = 0 \ , \tag{2.9}$$

$$\vec{h}_i \equiv \sum_j J_{ij} \langle \vec{s}_j \rangle \ . \tag{2.10}$$

We thus conclude that

$$\hat{n}_i = \hat{h}_i \tag{2.11}$$

for all i. Here $\hat{h}_i$ is the unit vector along $\vec{h}_i$. We call $\vec{h}_i$ the local field at the ith spin. Thus, this variational procedure is equivalent to treating the spins as classical vectors $\frac{1}{2}\hat{n}_i$. Each vector $\hat{n}_i$ must point along its local field $\vec{h}_i$. This is a "mean-field" theory. The solution to the problem of determining such $\hat{n}_i$'s is highly nontrivial. Walker and Walstedt[7] have performed numerical simulations and obtained the distribution of $\vec{h}_i$ for the ground state There is no guarantee that the numerical simulation can reach the truly lowest-energy spin configuration. However, at least a very low-energy metastable configuration can be obtained. This situation does reflect what is expected to happen in the laboratory. When the sample is cooled down to near-zero temperature, a low-energy metastable spin configuration is reached. This can be regarded as the ground state, for all practical purposes.

C. Excited states and metastability

If some of the spins are reversed, i.e., $\hat{n}_i = -\hat{h}_i$ for some i, we get an excited state. The excitation energy is h_i if the spin i is reversed.

This picture of localized excitation is not appropriate for the low-energy excited states, which instead involve the rotations of many spins through small angles. These extended excited states are the "spin waves." In quantum mechanics a spin-wave state is just a linear combination of single localized excitations over an extended region. Walker and Walstedt have in essence obtained the single-spin excited states numerically.[7] One of their conclusions was that the lower-energy states are more extended and the higher-energy ones are more localized.

We are more interested in the metastable states. In this model, transitions among energy levels are accomplished by H_{sl} [see Eq. (2.4)] which flips one spin at a time. A single-spin excitation thus cannot be metastable. We need to study states involving the reversal of at least two spins. A reasonable physical picture of a metastable state is as follows. Start with the ground state. A small nucleus of spins is reversed. Then the spins and the surrounding of these spins are readjusted to lower the energy. If a new configuration which is a new energy minimum is reached, we have a metastable state.

The height of the energy barrier is the most important characteristic of a metastable state. It determines the decay rate of the metastable state. In an Ising model such as that of Ref. 5, the barrier height is straightforward to calculate. But for the present model it is far more difficult. To illustrate this point, consider two spins $\vec{s}_1$ and $\vec{s}_2$. The part of energy involving them is

$$-\vec{h}_1 \cdot \vec{s}_1 - \vec{h}_2 \cdot \vec{s}_2 - J_{12} \vec{s}_1 \cdot \vec{s}_2 \ ,$$

where $\vec{h}_1$ and $\vec{h}_2$ summarize the effect of all other spins on $\vec{s}_1$ and $\vec{s}_2$. We expect a metastable state to appear if J_{12} is large compared to h_1 and h_2. When one of the spins $\vec{s}_1$ is flipped, the energy increases by about $h_1 + J_{12}$. When both are flipped, the net change of energy is $h_1 + h_2$. The barrier height is then $h_1 + J_{12}$ or $-h_2 + J_{12}$ whichever is smaller. We have assumed $J_{12} > 0$ for simplicity and have not kept track of angular dependence of energies. Clearly, if $h_2 > J_{12}$, there would be no metastable state. The same argument also shows that h_1 must be less than J_{12} in order to have a metastable state. These arguments were those used for the Ising model of Ref. 5. However, they are not quite applicable here because of the vector and quantum nature of the spins. For instance, if J_{12} is very large, one would conclude that the barrier height is very large, i.e., $\sim J_{12}$. This conclusion is incorrect. Very large J_{12} would make $\vec{s}_1$ and $\vec{s}_2$ stick together like a single spin 1. The total spin can be turned as a vector. The

barrier height cannot be as high as J_{12}. The vector nature of the spins and the long-range nature of the interaction also imply that the turning of the total spin $\vec{s}_1+\vec{s}_2$ would necessarily cause some readjustment of the surrounding spins. This situation does not occur for the Ising case of Ref. 5. Clearly, to make a precise determination of the barrier height and other properties of the metastable states, one must analyze many spins at the same time. To avoid this difficult task, we shall settle for a crude approximation for treating a strongly coupled pair as the "nucleus" of a cluster. The couplings of the neighboring spins to the pair are weaker, and provide a variable environment for the pair. This approach, which we present below, is reasonable because of the very wide distribution of J_{ij} peculiar to the $1/r^3$ law, as we shall discuss in more detail in Sec. III.

We begin by modifying the trial wave function (2.6) and write

$$\Psi=\prod_{kl}\psi_{kl}\prod_{i}\psi_i \ . \tag{2.12}$$

Here ψ_i is the same as was defined in Eq. (2.6), i.e., the single-spin wave function with $\langle\psi_i|\vec{s}_i|\psi_i\rangle=\frac{1}{2}\hat{n}_i$. The wave function ψ_{kl} is for the pair of spins k and l. It has to be parametrized by more parameters. We choose strongly interacting pairs only, i.e., those with small r_{kl}, or large $|J_{kl}|$. The spins which are not paired are included in the second product in Eq. (2.12). Minimizing the energy $\langle\Psi|H_0|\Psi\rangle$, we obtain a more elaborated mean-field approximation. We have each pair behaving as one unit at the presence of local fields provided by its neighbors. Each unpaired spin will line up along its local field as we discussed before.

We shall use this pair picture as a basis for estimating properties of the metastable excited states. A strongly coupled pair will behave as a spin 1 if it is in a triplet state or no spin if in a singlet state. We shall be concerned with only the triplet case.

We now proceed to study the energy levels of a two-spin system in a fixed environment as a part of the variational procedure.

Consider the Hamiltonian for the pair of spins $\vec{s}_1$ and $\vec{s}_2$ with large J:

$$H_{12}=-J\vec{s}_1\cdot\vec{s}_2-\vec{h}\cdot(\vec{s}_1+\vec{s}_2)-\vec{h}^*\cdot(\vec{s}_1-\vec{s}_2) \ , \tag{2.13}$$

where $\vec{h}$ and $\vec{h}^*$ are parameters, which can be related to the local fields at sites 1 and 2, contributed by all spins other than the pair

$$\vec{h}=\tfrac{1}{2}(\vec{h}_1+\vec{h}_2) \ , \quad \vec{h}^*=\tfrac{1}{2}(\vec{h}_1-\vec{h}_2) \ . \tag{2.14}$$

The pair has four energy levels. They can be expressed as functions of J, h, h^*, and ϕ, where ϕ is the angle between $\vec{h}$ and $\vec{h}^*$. For strong coupling, i.e., J large compared to h and h^*, the energies of the triplet states measured from $-\frac{1}{4}J$ are zeros of $\det|E+\frac{1}{4}J-H_{12}|$:

$$(E+h^{*2}\cos^2\phi/J)(E^2-h^2)+E^2h^{*2}\sin^2\phi/J=0 \ . \tag{2.15}$$

Since there is a large energy gap between the singlet and the triplet, no interesting effect is expected at low temperatures if $J<0$. Thus we shall simply drop all strongly coupled pairs with $J<0$, and consider only the triplet states for the case of $J>0$. Figure 4 depicts the energy levels in the triplet as a function of h as given by Eq. (2.15). For $h\gg h^{*2}/J$, and for $h\ll h^{*2}/J$ the three levels are, respectively,

$$\begin{aligned} E_0&\approx -h-h^{*2}\sin^2\phi/2J, && -h^{*2}/J-Jh^2\sin^2\phi/h^{*2} \ , \\ E_1&\approx -h^{*2}\cos^2\phi/J, && -h\cos\phi \ , \\ E_2&\approx h-h^{*2}\sin^2\phi/2J, && h\cos\phi \ . \end{aligned} \tag{2.16}$$

The three levels can also be derived from an effective Hamiltonian, with $\vec{s}=\vec{s}_1+\vec{s}_2$, operating in the triplet states,

$$H_{\text{eff}}=-h^{*2}/J+(\vec{h}^*\cdot\vec{s})^2/J-\vec{h}\cdot\vec{s} \ . \tag{2.17}$$

The lowest level, labeled by 0, is to be chosen for the ground state or for the metastable state. Note that $\vec{h}^*$ produces an anisotropy. Hence we call $\vec{h}^*$ "anisotropy field" and h^{*2}/J "anisotropy energy."

The state of the pair is characterized by the average values

$$\begin{aligned} \langle\vec{s}\rangle&\equiv\langle\vec{s}_1+\vec{s}_2\rangle=-\frac{\partial E_0}{\partial\vec{h}} \ , \\ \langle\vec{s}^*\rangle&\equiv\langle\vec{s}_1-\vec{s}_2\rangle=-\frac{\partial E_0}{\partial\vec{h}^*} \ . \end{aligned} \tag{2.18}$$

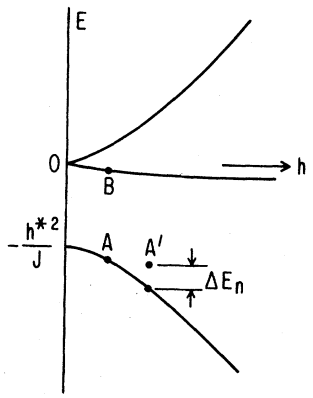

FIG. 4. Energy levels of the triplet states of a strongly coupled pair. [See Eqs. (2.15) and (2.16).]

For large h, i.e., $h \gg h^{*2}/J$, we have

$$\langle \vec{s} \rangle \approx \hat{h} \ , \qquad \langle \vec{s}^{\,*} \rangle \approx [\vec{h}^{\,*} - \hat{h}(\hat{h} \cdot \vec{h}^{\,*})]/J \ . \tag{2.19}$$

The total spin $\vec{s}$ is frozen along $\vec{h}$. For small h, i.e., $h \ll h^{*2}/J$, we have

$$\langle \vec{s} \rangle \approx 2J[\vec{h} - \hat{h}^{*}(\hat{h}^{*} \cdot \vec{h})]/h^{*2} \ , \qquad \langle \vec{s}^{\,*} \rangle \approx 2\vec{h}^{\,*}/J \ . \tag{2.20}$$

In this case, $\langle \vec{s} \rangle$ is small and $|\langle \vec{s}^{\,*} \rangle|$ assumes its maximum value. We may say that $\langle \vec{s}^{\,*} \rangle$ is frozen along $\vec{h}^{\,*}$.

The total energy of the system is

$$\langle \Psi | H_0 | \Psi \rangle = -\tfrac{1}{2} \sum_{i,j} J_{ij} \hat{n}_i \cdot \hat{n}_j + E_0(h, h^*, \phi) \ , \qquad \Psi = \psi_{12} \prod_i{}' \psi_i \ . \tag{2.21}$$

Here we keep only one pair, i.e., 12, in Eq. (2.12) for the simplicity of discussion. To minimize $\langle \Psi | H_0 | \Psi \rangle$, we must satisfy Eq. (2.11). The local field $\vec{h}_i$ given by Eq. (2.10) must now include $J_{i1}\langle \vec{s}_1 \rangle + J_{i2}\langle \vec{s}_2 \rangle$ which depends on $\vec{h}$ and $\vec{h}^{\,*}$. In addition, we must satisfy Eq. (2.14) with

$$\vec{h} = \tfrac{1}{2} \sum_i{}' (J_{1i} + J_{2i}) \hat{n}_i \ , \quad \vec{h}^{\,*} = \tfrac{1}{2} \sum_i{}^{*} (J_{1i} - J_{2i}) \hat{n}_i \ . \tag{2.22}$$

Suppose that we have carried out this program and determined the configuration $(\hat{n}_i, \vec{h}, \vec{h}^{\,*})$ for the ground state. How do we find a metastable state? Following the physical picture discussed above [Eq. (2.12)], the program would be as follows. Given the state A in Fig. 4, let us start with the state B, which is orthogonal to A but in general not satisfying the energy-minimum conditions. The next step is to make changes of $\hat{n}_i$ for the neighboring spins until Eqs. (2.11) and (2.22) are satisfied and the new configuration is a metastable state. The new environment of the pair will be described by new fields $(\vec{h}', \vec{h}^{\,*\prime})$ which would be very different from $(\vec{h}, \vec{h}^{\,*})$. Suppose that h is very small for the state A as indicated by Fig. 4. Thus $\langle \vec{s} \rangle_A$ is small. The average $\langle \vec{s} \rangle_B$ however has a magnitude unity and points along $\vec{h}^{\,*}$ (or $-\vec{h}^{\,*}$). The existence of a large $\langle \vec{s} \rangle$ will strongly affect the neighboring spins, which then rearrange to produce a field along $\langle \vec{s} \rangle$ to lower the energy. The final energy is

$$E' = E_0(h', h^{*\prime}, \phi') + \Delta E_n' \ , \tag{2.23}$$

where $\Delta E_n'$ is the change of interaction energy among the neighboring spins. It may be positive or negative. The new state is shown in Fig. 4 as A'.

If $E' > E_A$ then A' is a metastable. If $E' < E_A$ however, A should be called metastable instead. As Fig. 4 shows, a state of larger h has a lower energy. We therefore expect metastable states to have smaller h, and the stable states to have larger h. For very large h, it becomes unlikely to obtain a metastable configuration without reversing a large number of spins.

The important quantity is the barrier height Λ for a metastable state. From the above discussion, the only conclusion we can draw is that it is comparable to h^{*2}/J. The precise value of Λ depends on the behavior of the neighbors. Note that the difference in energy between the stable state and the metastable state may be large if E' of Eq. (2.23) involves many spins. However, the barrier height, which is the minimum energy required to initiate the decay of the metastable state, should not differ much from h^{*2}/J, the anisotropy energy for the pair.

It is important to note that the neighboring spins not only have energy, but also have a net spin, which changes as the state changes from the stable to the metastable.

D. Generalization to strongly coupled trios and larger nuclei, the energy tensor

The above analysis can be extended to include strongly and ferromagnetically coupled spin trios, and further to larger numbers of spins. If the couplings within the trio spins are very strong compared to couplings to other neighboring spins, then we shall get an "anisotropy energy tensor" to describe the total spin of the trio.

The variational trial wave function (2.12) can be further improved to include trios

$$\psi = \prod_i \psi_i \prod_{kl} \psi_{kl} \prod_{mnp} \psi_{mnp} \ . \tag{2.24}$$

The Hamiltonian involved in analyzing the energy involving a trio can be written in the following form. Consider spins $\vec{s}_1$, $\vec{s}_2$, and $\vec{s}_3$. We write

$$H_{123} = -J_{12}\vec{s}_1 \cdot \vec{s}_2 - J_{23}\vec{s}_2 \cdot \vec{s}_3 - J_{31}\vec{s}_3 \cdot \vec{s}_1 - \vec{h} \cdot (\vec{s}_1 + \vec{s}_2 + \vec{s}_3) - \vec{h}_1^{\,*} \cdot (\vec{s}_1 - \vec{s}_3) - \vec{h}_2^{\,*} \cdot (\vec{s}_2 - \vec{s}_3) \ . \tag{2.25}$$

This is a generalization of the H_{12} of Eq. (2.13). The parameters $\vec{h}$, $\vec{h}_1^{\,*}$, and $\vec{h}_2^{\,*}$ are related to the local fields $\vec{h}_1$, $\vec{h}_2$, and $\vec{h}_3$ via the relations $\vec{h}_1 = \vec{h} + \vec{h}_1^{\,*}$, etc. Here $\vec{h}_1$, $\vec{h}_2$, $\vec{h}_3$ are local fields contributed by sources *other than* the spins in the trio. Now we assume that the J's are large compared to $\vec{h}$ and the $\vec{h}^{\,*}$'s, and proceed with perturbation theory. We keep $\vec{h}$ to the first order and $\vec{h}^{\,*}$'s to the second order. The J's are assumed to be positive. Thus, in the zeroth-order approximation the ground states of H_{123}

are the four states of the quartet. The total spin is $\frac{3}{2}$. There are two doublets with energies higher than the ground state by amounts of the order of the J's. These doublets, like the singlet in the case of the pair discussed above, only play a role of the intermediate states in the second-order calculation of the energy.

Instead of calculating the energies directly, which involves much complicated algebra, we introduce, similar to Eq. (2.17), an effective Hamiltonian for the four states of the quartet. Define the operator $\vec{s} = \vec{s}_1 + \vec{s}_2 + \vec{s}_3$ operating in the space of the quartet only. One obtains

$$H_{\text{eff}} = E_0 + A(\vec{h}_1^* \cdot \vec{s})^2 + A(\vec{h}_2^* \cdot \vec{s})^2 + B[(\vec{h}_1^* \cdot \vec{s})(\vec{h}_2^* \cdot \vec{s}) + (\vec{h}_2^* \cdot \vec{s}_1)(\vec{h}_1^* \cdot \vec{s})] - \vec{h} \cdot \vec{s} \ . \quad (2.26)$$

The effective Hamiltonian is to reproduce the four energy levels in the quartet. The constants E_0, A, and B are functions of the J's. We give the detailed calculation in the Appendix, since we are only interested in the basic ideas. [See Eqs. (A16)–(A23).] The physical meaning of H_{eff} is clear. It sums up the dynamics of the trio, acting as a single spin $\frac{3}{2}$, with the effect of the environment approximately taken into account. Without looking at the energy levels in detail, we can already get a qualitative picture of the energies involved from H_{eff} directly. The effect of the field $\vec{h}$ is quite clear. No discussion is needed. The effect of $\vec{h}_1^*$ and $\vec{h}_2^*$ is to introduce anisotropy. We can write H_{eff} as

$$H_{\text{eff}} = E_0 + K_{\mu\nu}^* s_\mu s_\nu - \vec{h} \cdot \vec{s} \ , \quad (2.27)$$

where $K_{\mu\nu}^*$ is a symmetric tensor and $\vec{h}$ a vector which follow directly from Eq. (2.26), and $\mu, \nu = x,y,z$, summed if repeated. The symmetric tensor $K_{\mu\nu}^*$ has three principal axes and is best represented by an ellipsoid with these principal axes and radii equal to the three eigenvalues of $K_{\mu\nu}^*$. If $\vec{s}$ were a classical vector of fixed length, then, in the ground state and if $\vec{h} = 0$, $\vec{s}$ would be parallel or antiparallel to the principal axis with the lowest eigenvalue. There are two energy minima on the ellipsoid, i.e., where this principal axis intersects the ellipsoid surface. The barrier height is the difference between the two low eigenvalues. If $h \neq 0$ but fairly small, then these two minima would move away a bit. One of the energy minima would have a higher energy than the other, and would be a metastable state. Clearly, if h is larger than some critical value, then there will be only one energy minimum.

The fact that $\vec{s}$ is a quantum-mechanical operator complicates the picture. We have to essentially calculate the wave functions of $\vec{s}$ on the ellipsoid by diagonalizing H_{eff}. The simple arguments given above will be modified but the qualitative picture remains.

Clearly, we can generalize the above analysis to study a larger number of spins coupled by large and positive J's. The form of the effective Hamiltonian (2.26) will remain. $K_{\mu\nu}^*$ will be quadratic in many $\vec{h}^*$'s and are complicated functions of the J's. No matter how complicated these functions are, the qualitative picture of the ellipsoid and energy minima remain. This picture is not too different from that given by the "anisotropy" hypothesis often used in the phenomenological analysis of experimental data in micromagnetic domains.

Note that for the case of a pair, there is only one $\vec{h}^*$ and $K_{\mu\nu}^* = h_\mu^* h_\nu^* / J$. The ellipsoid is a "needle." Two principal radii are zero. For the trio, it is an elliptic "pancake." One principal radius is zero [see Eqs. (A25) and (A26)]. For a nucleus of more than three spins, all radii are in general nonzero.

The readjustment of neighbors due to a change of the total spin $\vec{s}$ for the trio and larger nuclei would be quite similar to that in the case of the pair discussed earlier. The energy of the metastable state and the barrier height must include the contributions from the neighbors.

E. Summary of the mean-field approximation

We started with a variational approximation with a trial wave function which is a product of single-spin wave functions. This allows us to define the local fields for single spins. Then we generalize the approximation to include strongly coupled pairs, each of which has an additional local field $\vec{h}^*$. This anisotropy field allows us to describe metastability. The pair acts as a nucleus for a cluster. The pair approach is naturally extended to trio and larger nuclei. The total spin of the nucleus is now described by the tensor $K_{\mu\nu}^*$, which is a quadratic function of two or more local fields analogous to the $\vec{h}^*$ for the pair, and a vector $\vec{h}$ which couples to the total spin. The tensor $K_{\mu\nu}^*$ follows the second-order perturbation calculation in the local fields, and describes the "anisotropy energy" for the nucleus.

Note that a pair does not have a metastable state for a rigid environment. Readjustment of neighbors is necessary. For trios and larger nuclei, metastable states are possible even with rigid neighboring spins. It should be emphasized that the neighboring spins are far from being rigid. The variational calculation must include the neighboring spins self-consistently.

This concludes our discussion of the basic physical picture of the spin-glass structure.

III. STATISTICS

In principle, one could calculate the distribution functions of the local fields $\vec{h}_i$ and hence those of other quantities of interest by solving the variational problem outlined in Sec. II. No such calculation is

attempted here. We shall only make rough estimates based on plausibility arguments.

A. Random spin approximation

Let us ignore the nuclei for the moment. We shall obtain an approximation to the distribution of the local field $\vec{h}_i$ by assuming random orientations for average spins $\langle \vec{s}_j \rangle$ which produce $\vec{h}_i$ [see Eq. (2.10)]. Corrections to this approximation will then be discussed.

We define $P(\vec{h})$ as the distribution, normalized to one, for the local field

$$P(\vec{h}) = \left\langle \delta\left[\vec{h} - \sum_j J_{ij}\hat{n}_j/2\right]\right\rangle , \tag{3.1}$$

where the average is taken over the positions $\vec{r}_j$, $(J_{ij} = \pm 4/|\vec{r}_i - \vec{r}_j|^3)$. Assume random orientation $\hat{n}_j$. We obtain

$$P_0(\vec{h}) = \tfrac{2}{3}[(\tfrac{2}{3}\pi^2) + h^2]^{-2} . \tag{3.2}$$

The details of the algebra leading to Eq. (3.2) may be of interest to some readers and are included in the Appendix.

The dashed curve of Fig. 5 represents $4\pi h^2 P_0(h)$. It peaks at

$$h_P = \tfrac{2}{3}\pi^2 = 6.58 . \tag{3.3}$$

Note that $\frac{1}{2}J/r^3 = 2$ for $r = 1$ and $J = 4$. [Remember our units given by Eq. (2.5).] If we say that there are 10 neighbors each producing a field of random sign of magnitude 2, then we would expect a fluctuation of $2\sqrt{10} \approx 6$, which is about the same size as Eq. (3.3).

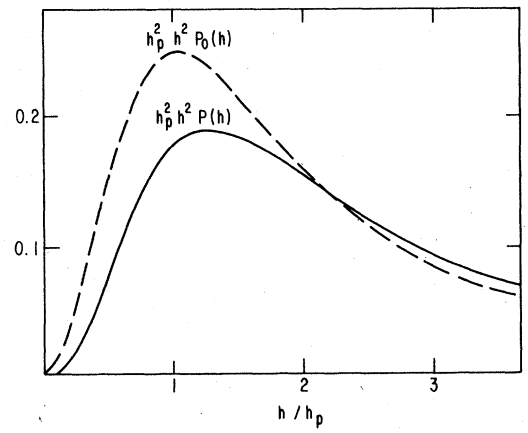

FIG. 5. Plot of $h^2P_0(h)$ (dashed curve) and $h^2P(h)$ (solid curve). See Eqs. (3.2) and (3.15). The cavity is not as dramatic here as in Fig. 1(a) because of the h^2 factor. $h_p = \frac{2}{3}\pi^2$.

Note that for large h

$$4\pi h^2 P_0(\vec{h}) \approx \tfrac{8}{3}\pi h^{-2} . \tag{3.4}$$

This implies a logarithmically divergent $\langle h \rangle$ and linearly divergent $\langle h^2 \rangle$. The reason is that the model allows spins to get so close to each other that $1/r_{ij}^3$ can become very large. If we impose a cutoff r_0 and exclude $r_{ij} < r_0$, then the large-h behavior will be altered. We obtain

$$P_0(\vec{h}) \approx (2\pi\mu_0^2)^{-3/2} e^{-h^2/2\mu_0^2} , \qquad \mu_0^2 \equiv \tfrac{8}{9}\pi h_0 , \quad h_0 \equiv 2/r_0^3 . \tag{3.5}$$

The detailed algebra is included in the Appendix. This result can be understood in view of the central limit theorem. $\langle h^2 \rangle$ can be calculated directly:

$$\begin{aligned} \langle h^2 \rangle &= \sum_{j,k} \langle J_{ij}J_{ik}\hat{h}_j \cdot \hat{h}_k \rangle /4 \\ &= \tfrac{1}{4}\sum_j \langle J_{ij}^2 \rangle \\ &= \tfrac{1}{4}\int_{r_0}^{\infty} 4\pi r^2 \, dr \left(\frac{4}{r^3}\right)^2 \\ &= 3\mu_0^2 . \end{aligned} \tag{3.6}$$

The same result also follows from Eq. (3.4):

$$\langle h^2 \rangle \approx \tfrac{8}{3}\pi \int_0^{h_0} \frac{dh}{h^2} h^2 = \tfrac{8}{3}\pi h_0 = 3\mu_0^2 . \tag{3.7}$$

The average $\langle h \rangle$ is more difficult to calculate since it depends on the intermediate range of h too, but

$$\langle h \rangle \approx \tfrac{8}{3}\pi \ln\mu_0$$

or (3.8)

$$\langle h \rangle \approx \mu_0\sqrt{8/\pi}$$

from Eqs. (3.4) or (3.5) should be a reasonable estimate.

B. Corrections to the random spin approximation

Now the question is how good the approximation (3.2) is. Let us discuss the most obvious implications of the energy-minimum condition (2.11), that each spin must point along its local field.

First we note that $P(\vec{h})$ must vanish at $\vec{h} = 0$, contrary to what Eq. (3.2) says. The reason is as follows. Suppose that $\vec{h}_i = 0$. Then a small rotation of a neighboring spin to $\hat{n}_j + \Delta\hat{n}_j$ would produce a local field $\vec{h}_i = J_{ij}\Delta\hat{n}_j$. This would produce an energy

change $\Delta E = -|J_{ij}\Delta\hat{n}_j|$ and contradicts the energy-minimum condition that ΔE must be of $O((\Delta\hat{n})^2)$ and positive. Therefore no $\vec{h}_i$ can be zero.

The above argument can be extended to estimate the correction to $P_0(\vec{h})$. Let $\vec{h}_1$, $\vec{h}_2$ be the local fields at sites 1 and 2. Let $\vec{h}'_1$ and $\vec{h}'_2$ be the contributions to $\vec{h}_1$ and $\vec{h}_2$ from spins other than $\vec{s}_1$ and $\vec{s}_2$. Thus

$$\vec{h}_1 = \vec{h}'_1 + \tfrac{1}{2}J_{12}\hat{h}_2 \ , \quad \vec{h}_2 = \vec{h}'_2 + \tfrac{1}{2}J_{12}\hat{h}_1 \ . \tag{3.9}$$

To minimize energy $\vec{h}_1$, $\vec{h}_2$, $\vec{h}'_1$, and $\vec{h}'_2$ must all lie in the same plane. Let θ and θ' be the angle between $\hat{h}_1$ and $\hat{h}_2$ and that between $\hat{h}'_1$ and $\hat{h}'_2$, respectively. Both θ and θ' are less than π.

From Eq. (3.9) we see that

$$\begin{aligned}\vec{h}'_1 \times \vec{h}'_2 &= h'_1 h'_2 \sin\theta' \hat{e}_z \\ &= \vec{h}_1 \times \vec{h}_2 - \tfrac{1}{4}J_{12}^2 \hat{h}_1 \times \hat{h}_2 \\ &= (h_1 h_2 - \tfrac{1}{4}J_{12}^2)\sin\theta \hat{e}_z \ ,\end{aligned} \tag{3.10}$$

where $\hat{e}_z$ is the unit vector along $\hat{h}_1 \times \hat{h}_2$. It follows that

$$h_1 h_2 - \tfrac{1}{4}J_{12}^2 = h'_1 h'_2 \sin\theta'/\sin\theta > 0 \ . \tag{3.11}$$

This must be true for any pair. Thus

$$h_i h_j > \tfrac{1}{4}J_{ij}^2 \tag{3.12}$$

for all i,j. This is a rather restrictive condition. Using this condition, we can estimate the correction to $P_0(h)$ as follows. Given $\vec{h}_i = \vec{h}$, the restriction in the space of all $\vec{h}_j$ imposed by Eq. (3.12) is

$$\prod_j \Theta(h_j - J_{ij}^2/4h) \ . \tag{3.13}$$

The smaller h, the stronger the restriction. We now take the average of this product over the random distribution of h_j (i.e., over P_0) and write the corrected distribution as

$$\begin{aligned}P(h) &\propto P_0(h)\prod_j g\left(\frac{J_{ij}^2}{4h}\right) \ , \\ g(h') &\equiv \langle\Theta(h_j - h')\rangle = \int_{h'}^{\infty} dh_j P_0(h_j) \ .\end{aligned} \tag{3.14}$$

Carrying out the algebra, we find that a "cavity" is created around $h = 0$ (see Fig. 1).

$$P(h) \approx P_0(h)C_0(h) \ , \quad C_0(h) \approx 1.8e^{-2.3/\sqrt{h}} \ . \tag{3.15}$$

The solid curve in Fig. 5 gives $4\pi h^2 P(h)$. We see that compared to $4\pi h^2 P_0(h)$ the maximum of the curve differs by about 20%. The small h part is suppressed. The large h part becomes larger as required by normalization.

When a cutoff is taken into account, the large h behavior [Eq. (3.5)] is also modified by the energy-minimum condition. An estimate of the modification can be made by keeping the $j \neq k$ terms in Eq. (3.6). Since there is a nonzero average of $J_{ik}\hat{h}_k$ along $\hat{h}_i$, we write

$$\begin{aligned}\langle h^2\rangle &= \tfrac{1}{4}\sum_{jk}\langle J_{ij}J_{ik}\hat{h}_j\cdot\hat{h}_k\rangle = \left\langle\tfrac{1}{2}\sum_j (J_{ij}\hat{h}_j)\right\rangle\cdot\hat{h}_i\left\langle\tfrac{1}{2}\sum_k (J_{ik}\hat{h}_k)\right\rangle\cdot\hat{h}_i \\ &\quad + \tfrac{1}{4}\sum_j\langle J_{ij}^2[1-(\hat{h}_i\cdot\hat{h}_j)^2]\rangle = \langle h_i\rangle^2 + \tfrac{1}{4}\sum_j\langle J_{ij}^2[1-(\hat{h}_i\cdot\hat{h}_j)^2]\rangle\end{aligned} \tag{3.16}$$

since $\vec{h}_i = \sum_j J_{ij}\hat{h}_j$. Now we take the average over Eq. (3.5) to obtain

$$\langle h^2\rangle = \mu_0^2(8/\pi) + 2\mu_0^2 = 3\mu_0^2(1.52) \ . \tag{3.17}$$

This implies that μ_0^2 is increased by 1.5 as a result of the energy-minimum condition.

Note that one can also estimate $\langle h^2\rangle$ using Eq. (3.15) for large h:

$$\langle h^2\rangle \approx \int_0^{h_0} 4\pi h^2 \frac{2}{3h^4}(1.8)h^2 dh = 3\mu_0^2(1.8) \tag{3.18}$$

which is in reasonable agreement with Eq. (3.17).

C. Distribution of $\vec{h}$ and $\vec{h}^*$

Now we proceed to discuss the statistics of $\vec{h}$ and anisotropy fields $\vec{h}^*$ of a strongly coupled pair or a larger nucleus. Without a much more elaborated analysis, it is difficult to give a precise criterion for "strong" coupling. Fortunately, we can easily estimate the number of nuclei with J larger than a given J_m. Note that e^{-v} is the probability of finding no other spin in a volume v around a given spin. Therefore the probability that a given spin is coupled to at least one other spin with coupling larger than J_m is

$$p(J_m) = \tfrac{1}{2}(1 - e^{-v}), \quad v \equiv \tfrac{4}{3}\pi(4/J_m) \ , \tag{3.19}$$

where the factor $\frac{1}{2}$ is to exclude negative J. For

$\frac{1}{4}J_m = 5, 10$ we have $p = 28\%$ and 17%, respectively. This tells us that there are plenty of nuclei and the distribution of J is very wide.

For a given pair, the distribution of $\vec{h}$ and $\vec{h}^*$, $P(\vec{h}, \vec{h}^*)$, can be calculated approximately by assuming random and independent orientations of the surrounding spins. The calculation is similar to that for $P_0(\vec{h})$ and we leave the details in the Appendix. We have

$$P(\vec{h}, \vec{h}^*) \approx \bar{P}_0(h)\bar{P}_0(h^*) \ , \tag{3.20}$$

where the function $\bar{P}_0$ is given by

$$\bar{P}_0(\vec{h}) \approx \tfrac{1}{3}[(\tfrac{1}{3}\pi^2)^2 + h^2]^{-2} \tag{3.21}$$

for small h and

$$\bar{P}_0(\vec{h}^*) \approx (\pi J/\alpha)^{-3/2} e^{-\alpha h^{*2}/J} \ , \quad \alpha = \tfrac{9}{8}\pi \ , \tag{3.22}$$

for large h^*. There is an additional simplification made in deriving these results. The distance $|\vec{r}_1 - \vec{r}_2|$ between the two spins of the pair is assumed to be small compared to the distance to other spins. This simplification makes $\vec{h}$ and $\vec{h}^*$ independent. [See Eqs. (A11) and (A13).] Each neighbor either contributes to $\vec{h}$ or to $\vec{h}^*$ but not both. We have chosen the cutoff $h_0 = J$, i.e., excluded the cases where the surrounding spin is too close to the pair. $\bar{P}_0(h)$ is simply $P_0(h)$ with a change of scale [see Eqs. (3.2) and (3.5)].

The extension of these calculations to trios and larger nuclei is straightforward but involving many J's and $\vec{h}^*$'s. Since we are only making a qualitative estimate, we shall simply apply the above results to all nuclei. h^* is taken to be a typical anisotropy field and $\vec{h}^{*2}/J$ a typical anisotropy energy for any nucleus.

There are also corrections to P due to the energy-minimum condition, as there was in the single-spin case. This correction should not be as large as in the single-spin case since a pair can have its ground state with $h = 0$ as long as $h^* \neq 0$. The cases with both h and h^* small is not very significant statistically. However, we do expect that a nucleus with small h is more likely to be found in a metastable state of the system. The decay of metastable states will therefore modify the distribution of h. This is discussed next.

D. Distributions involving the metastable states

If $h^* = 0$, then the nucleus would have no metastable state. According to our arguments in Sec. II, h^* is essential to keep a nucleus with small h from reorienting itself and increasing h. For very small h^*, we therefore expect that the distribution for h would be $\bar{P}_0(h)$ multiplied by a cavity factor similar to $C_0(h)$ of Eq. (3.15) but not vanishing at $h = 0$ since any nonvanishing h^* would produce some metastability. The decay of metastable states would make the cavity deeper. Some decays occurred while the system was being cooled from a higher temperature before the observation. Fig. 1(b) showed what one would expect for the distribution of $\vec{h}$.

We shall need information concerning the distributions for various quantities for our calculations in the following sections. We now make the following estimates and assumptions based on the above discussion and the analysis of Sec. II.

(i) The barrier height Λ is of the order of h^{*2}/J. We write

$$\Lambda = h^{*2}/J + \Lambda' \ , \tag{3.23}$$

where Λ' is expected to have a probability distribution extended a bit toward the negative side. Since Λ' simply smears up the distribution to a limited extent, we shall drop it for simplicity of discussion. The smearing due to Λ' can always be put in at the end of a calculation without difficulty. Dropping Λ' we obtain a simple estimate of the barrier height distribution

$$\rho(\Lambda) \equiv \int d^3h^* \bar{P}_0(h^*) \delta\left(\Lambda - \frac{h^{*2}}{J}\right)$$

$$\approx (\alpha/\pi)^{3/2} 2\pi\sqrt{\Lambda} e^{-\alpha\Lambda} \ . \tag{3.24}$$

We have used Eq. (3.22) for $\bar{P}_0(h^*)$ since the contribution comes from large $h^* \sim \sqrt{J}$. Near $\Lambda = 0$, the smearing due to Λ' of Eq. (3.23) would wash out the square-root singularity.

(ii) We expect that there are more metastable nuclei with small h. Therefore we assume that the decay of metastable states will gradually create a cavity on the distribution of h centered at $h = 0$. What is more important is the cavity shape function C before any substantial decay of metastable states, i.e., the "initial" cavity shape. Clearly, C depends on how the system is prepared. We have to make special assumptions about C for each case of interest. The important overall assumption is that C would change slowly with a characteristic rate $\gamma = (1/\tau)e^{-\Lambda/T}$, which will be discussed further in Sec. IV.

(iii) We set

$$\langle \vec{s} \rangle = \begin{cases} \hat{h}, & \text{for } h > h^{*2}/J, \\ \vec{h}J/h^{*2} = \vec{h}/\Lambda, & \text{for } h < h^{*2}/J. \end{cases} \tag{3.25}$$

This is an approximation to Eqs. (2.19) and (2.20) for the spin of the pair.

These estimates [Eqs. (3.23)–(3.25)] involve two characteristic energies: the field energy h and the anisotropy energy h^{*2}/J. They should apply qualitatively to all nuclei.

IV. DECAY OF METASTABLE STATES

A. Transition rates

The effect of the term H_{sl} [see Eqs. (2.1) and (2.4)] in the Hamiltonian is to cause transitions among the eigenstates of H_0. A transition is "allowed" if the transition amplitude is nonzero to first order in H_{sl}. Otherwise the transition is "forbidden." Only single-spin-flip transitions are allowed. We shall not enter into any of the details of the spin-lattice interaction. We simply regard all single-spin-flip rates as approximately equal to some constant $1/\tau$. The characteristic time τ is regarded as a microscopic time, (computable by applying the Fermi's "golden rule" to H_{sl}), even though H_{sl} is assumed to be very weak.

The more interesting transitions are the higher-order transitions, i.e., the forbidden transitions between metastable and stable states, involving the flipping of two or more spins. The flipping of a nucleus of spins is a higher-order process. The rate can be calculated with H_{sl}. Such a rate is expected to be extremely small. One reason is that H_{sl} is small. The other reason is that the final state is very different from the initial state because of the readjustment of many neighboring spins. Therefore, we expect that the forbidden process must be accomplished by a succession of independent allowed transitions, rather than by a single high-order process. In other words, we exclude the quantum-mechanical tunneling as a mechanism for the decay or activation of metastable states. The spins are flipped one by one. The energy barriers which make the states metastable must be overcome by thermal activation.

The most important factor in the decay rate of the metastable state via successive transitions over the barrier is $e^{-\Lambda/T}$, where Λ is the barrier height. For our qualitative discussion here, we shall simply ignore other details of the transitions and write the decay rate as

$$\gamma(\Lambda) = (1/\tau)e^{-\Lambda/T} \quad . \tag{4.1}$$

B. Integrations over $e^{-\gamma t}$

In calculating various quantities of interest involving the metastable states, one encounters integrals of the form

$$I(t) = \int_0^\infty d\Lambda g(\Lambda) e^{-\gamma(\Lambda)t} \quad , \tag{4.2}$$

where γ is given by Eq. (4.1). It should be helpful to learn the basic feature of such an integral before applying it.

We write

$$\begin{aligned} \gamma t &= (t/\tau)e^{-\Lambda/T} \\ &= \exp\{-[\Lambda - T\ln(t/\tau)]/T\} \\ &\equiv e^{-(\Lambda - x)/T} \quad , \\ x &\equiv T\ln(t/\tau) \quad . \end{aligned} \tag{4.3}$$

Clearly, γt is very large for $\Lambda << x$ and very small for $x << \Lambda$. For very small T, $e^{-\gamma t}$ therefore behaves like a step function. It is zero for $\Lambda < x$ and 1 for $\Lambda > x$. The region of transition from 0 to 1 has a width of about T. Thus we have for small T

$$e^{-\gamma t} \approx \Theta(\Lambda - x) = \Theta(\Lambda - T\ln(t/\tau)) \quad . \tag{4.5}$$

This simply says that the metastable states with barriers lower than x have decayed and those with barriers higher than x remain. The integral (4.2) is therefore simply

$$I(t) \approx \int_x^\infty d\Lambda g(\Lambda), \quad \int_0^\infty d\Lambda g(\Lambda) e^{-\gamma t} \approx \int_{T\ln(t/\tau)}^\infty d\Lambda g(\Lambda) \quad . \tag{4.6}$$

This a very useful formula. It is a good approximation if $g(\Lambda)$ does not change much when Λ changes by T. Clearly, this is useful only for $t/\tau >> 1$. $I(t)$ is the area under $g(\Lambda)$ to the right of $x = T\ln(t/\tau)$ (see Fig. 6). The part to the left has decayed. For positive g, I is always a decreasing function of x. For example, if $g(\Lambda) = e^{-a\Lambda}$, we have simply

$$I(t) = \frac{1}{a}e^{-ax} = \frac{1}{a}\left(\frac{t}{\tau}\right)^{-aT} \quad . \tag{4.7}$$

Even if $g(\Lambda)$ has ups and downs, the integral I will be smoother and decreasing as a function of x. For small T it would remain a down-sloping straight line in the plot I vs ln (t) for a wide range.

From the derivation, it is clear that the formula (4.6) is valid for small T even if we multiply γ by a smooth function of Λ. The change can be regarded simply as a change of τ. Since τ appears in the logarithm, it has very little effect.

It is important to note that the magnitude of τ of experimental interest is of the order of the spin-lattice relaxation time $\tau \sim 10^{-10}$ sec. The macroscop-

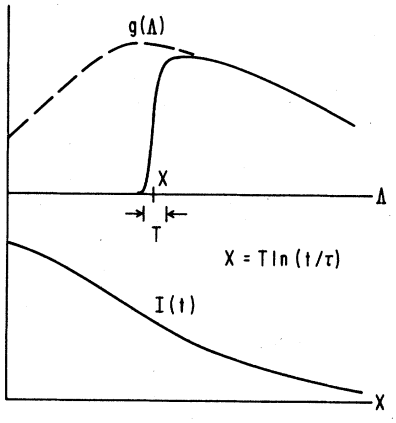

FIG. 6. The factor $e^{-\gamma t}$ is approximately a step function $\Theta(\Lambda - T\ln(t/\tau))$. The integral $I(t)$ [see Eq. (4.2)] is the area under the solid curve.

ic time scale is $t \sim 10$ sec. Thus $\ln(t/\tau) \sim 25$. For $T/T_c \sim 0.1$, $(T/T_c)\ln(t/\tau)$ is not a small number.

V. MAGNETIC SUSCEPTIBILITY

When an external magnetic field $\vec{h}_A$ is turned on, a total magnetization appears. A part of this magnetization appears very fast. We shall discuss it first. There is also a part, which involves the metastable states, and appears very slowly after the field is turned on.

A. Fast response

When the applied field $\vec{h}_A$ is turned on, the local field is changed for each spin. If $\vec{h}_A$ is turned on not too abruptly, each spin will follow the field and ends up in the direction of its new local field, according to the "adiabatic theorem" of quantum mechanics. What is needed now is the distribution function for the new local fields. A reasonable estimate is

$$P'(\vec{h}) = P_0(\vec{h} - \vec{h}_A)C_0(h) \ , \tag{5.1}$$

where $C_0(h)$ is the cavity factor $\sim e^{-2.3/\sqrt{h}}$ given by Eq. (3.15) and P_0 given by Eq. (3.2). The applied field shifts all local fields by $\vec{h}_A$. That is why the argument of P_0 is replaced by $\vec{h} - \vec{h}_A$. On the other hand, the factor $C_0(h)$ comes from the adjustment of spins to reach an energy minimum. This process of adjustment is completed only after the field is turned on. The discussion leading to C_0 [see Eqs. (3.9)–(3.15)] was independent of any applied field. Therefore the argument of C_0 must be $\vec{h}$, not $\vec{h} - \vec{h}_A$. The average spin is then

$$\vec{m} = \int d^3h P_0(\vec{h} - \vec{h}_A)C_0(h)\frac{\hat{h}}{2}$$
$$= -\int d^3h\, \vec{h}_A \cdot \hat{h}\frac{\partial P_0}{\partial h}C_0(h)\frac{\hat{h}}{2} \ .$$

From this we obtain the susceptibility per spin

$$\chi_1 = \vec{m}\cdot\hat{h}_A/h_A \approx 0.03 \ . \tag{5.2}$$

Note that the high-temperature susceptibility (Curie law) is

$$\chi^{\text{Curie}} = 1/4T \ . \tag{5.3}$$

Since we expect the spin-glass transition temperature T_c to be of the order of magnitude unity, we see that χ_1 given by Eq. (5.2) is a small fraction of the susceptibility at the transition temperature.

Frozen neighbors are assumed in arriving at Eq. (5.2). The neighbor spins do change under $\vec{h}_A$ and thereby change $\vec{h}_i$. However, due to the random signs of J_{ij}, the resulting change in $\vec{h}_i$ is expected to be random and thereby not affecting Eq. (5.2). A part of the spin readjustment is taken care of by the fact that the cavity factor $C_0(h)$ does not follow $\vec{h}_A$.

The response of a nucleus of Z spins to $\vec{h}_A$ is very different from that of Z single spins each in a frozen field. We need to calculate the susceptibility contributed by a nucleus by treating the nucleus as a single unit. When $\vec{h}_A$ is turned on, $\vec{h}$ is changed into $\vec{h} + \vec{h}_A$ but $\vec{h}^*$ is unchanged if we ignore the decay of metastable states. Thus the average magnetization per nucleus is

$$\vec{m} = \int d^3h d^3h^* P(\vec{h} - \vec{h}_A, \vec{h}^*)\langle\vec{s}\rangle \ , \tag{5.4}$$

where $\langle\vec{s}\rangle$ is the total spins given $\vec{h}$ and $\vec{h}^*$ [see Eq. (3.25)]. The susceptibility per nucleus is then

$$\chi_N = -\tfrac{1}{3}\int d^3h d^3h^* \frac{\partial \bar{P}_{0(h)}}{\partial h}|\langle\vec{s}\rangle|\bar{P}_0(h^*) \approx 0.04 \ , \tag{5.5}$$

where we have used Eqs. (3.21) and (3.22) for evaluating the integral. This result has not included the effect of the decay of metastable states. As we have mentioned earlier, the stable states have larger total spins. Therefore, we expect χ_N to increase as more metastable pairs decay. We now turn to this effect.

B. Time-dependent part of the susceptibility

The decay of the metastable states will introduce a time-dependent part of the susceptibility. The reason

can be seen from Fig. 7. The center of the distribution is shifted from 0 to $\vec{h}_A$ after the field is turned on. The decay of metastable states will move the cavity back toward zero. This will increase the net spin and hence the susceptibility. The cavity would also increase in depth as more metastable states decay, but the contribution to the net average spin comes only from the asymmetry of the cavity.

We estimate the cavity factor as follows. Ignore the applied field h_A for the moment and imagine that the system is cooled down from a high temperature. When the temperature reaches T_m, the metastable states freeze. T_m should be about the same as T_c, the transition temperature. Metastable states with very high barriers would freeze a little earlier and those with low barriers freeze a little later. As the temperature drops further and before waiting for very long, the metastable states follow the distribution $\exp(-E/T_m)$, with

$$E \approx E_n - h^2 J/2h^{*2} \approx E_n - h^2/2\Lambda \ . \tag{5.6}$$

Here E_n denotes the energy of the neighbors and the h^2 term is the energy of the nucleus [see Eq. (2.16)]. In other words, the distribution is frozen at the equilibrium distribution of T_m. Ignoring the correlation of E_n with h, we arrive at the following estimate for the cavity factor. For $h < \Lambda$

$$C(h) \approx e^{h^2/2\Lambda T_m} e^{-\Lambda/2T_m} \tag{5.7}$$

and $C(h) = 1$ for $h > \Lambda$. This factor is normalized so that $C(\Lambda) = 1$.

After the field $\vec{h}_A$ is applied, how would the cavity change? We simply take the new shape as $C(\vec{h} - \vec{h}_A)$ since all local fields change by $\vec{h}_A$ if $\vec{h}_A$ is small enough. There is an additional correction to $C(\vec{h} - \vec{h}_A)$ because the neighborhood would also change with $\vec{h}_A$. For small $\vec{h}_A$, this change can be estimated from Eq. (5.6):

$$E_n(\vec{h}_A) \approx -\vec{h}_A \cdot \langle \vec{s}_n \rangle + E_n(0) \ , \tag{5.8}$$

since the derivative of E_n with respect to an applied field is just the net average spin $\langle \vec{s}_n \rangle$ of the neighbors. Thus, the new cavity factor is

$$C'(\vec{h}) = C(h) + \frac{\vec{h}_A}{T_m}\left(\frac{\vec{h}}{\Lambda} + \langle \vec{s}_n \rangle\right) e^{h^2/2\Lambda T_m} e^{-\Lambda/2T_m} \ . \tag{5.9}$$

Clearly $\vec{h}/\Lambda + \langle \vec{s}_n \rangle$ is just the total spin of the nucleus and its neighbors. The symmetric term $C(h)$ does not contribute to the net magnetization. The asymmetric term will decay in time. Using the barrier height distribution (3.24), we obtain the time varying part of the susceptibility

$$\chi^*(t) = -\int_0^\infty d\Lambda g(\Lambda) e^{-\gamma t} \ , \tag{5.10}$$

$$g(\Lambda) = \frac{1}{T_m}\left(\frac{2}{3}\pi\right)\left(\frac{\alpha}{\pi}\right)^{3/2} \sqrt{\Lambda} e^{-\alpha\Lambda} \int d^3h \bar{P}_0(h)\left(\frac{h^2}{\Lambda^2} + \frac{n}{4}\right)\Theta(\Lambda - h) \exp[-(\Lambda^2 - h^2)/2\Lambda T_m] \ . \tag{5.11}$$

We have replaced $\langle\langle s_n \rangle^2\rangle$ by $\frac{1}{4}n$ and dropped $\langle\langle s_n \rangle\rangle$. Here the second average is over all the pairs and n is the mean number of neighboring spins which rearrange following the decay of the metastable state.

The function $g(\Lambda)$ is plotted in Fig. 8. It is calculated with $T_m = 1$ and $n = 10$. Figure 2 shows χ^* obtained from Eq. (5.10) versus $x \equiv T \ln(t/\tau)$. The magnitude of χ^* is roughly proportional to T_m and n but the variation in x is roughly independent of these parameters. Note that χ^* is negative. It is flat for small x and decays to zero for large x. Comparison with experimental results will be discussed in Sec. VII.

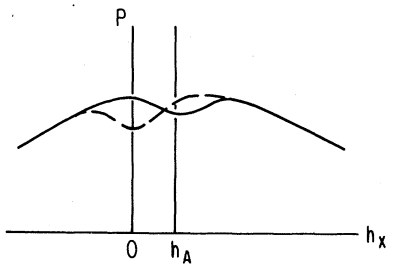

FIG. 7. The external field shifts the whole distribution to the right. The cavity will slowly move back to the center toward the dashed curve, due to decays of metastable states.

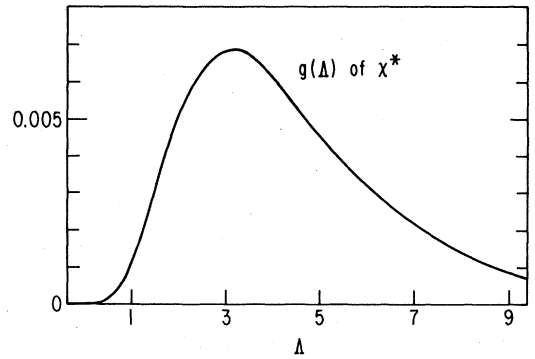

FIG. 8. The function $g(\Lambda)$ for χ^* [see Eq. (5.10)], evaluated for $T_m = 1$ and $n = 10$.

VI. REMANENT MAGNETIZATION

A. General considerations

The remanent magnetization is the macroscopic magnetization which remains after the applied field $\vec{h}_A$ has been turned off. Its magnitude depends on h_A and also depends on how the sample was prepared and how h_A was applied. Two cases are of current experimental interest: (i) the thermal remanent magnetization (TRM), and (ii) the isothermal remanent magnetization (IRM). In the case of TRM, the sample is cooled to the low temperature T from above the spin-glass transition temperature T_c at the presence of $\vec{h}_A$. Then one turns $\vec{h}_A$ off. For IRM, the sample is cooled to T without $\vec{h}_A$. One then turns on $\vec{h}_A$ for some time. Then one turns it off.

Clearly, the existence of the remanent magnetization reflects the existence of metastable states. We shall examine how the metastable states behave under the TRM and IRM conditions in our simple picture.

For a nucleus in the fields $\vec{h}$ and $\vec{h}^*$, the application of $\vec{h}_A$ changes $\vec{h}$ to $\vec{h}+\vec{h}_A$ but does not change $\vec{h}^*$, as we learned earlier. However, there are additional complications when h_A is or was large enough to produce a sizable magnetization, which then produces changes of local fields through the exchange couplings. These changes of local fields are largely random since J_{ij} are random. But it seems entirely reasonable to expect some asymmetry in the distribution of the random changes since there is a preferred direction $\vec{h}_A$. For simplicity we shall ignore this complication.

We expect that as $\vec{h}_A$ is turned on or off smoothly, the total spin $\langle \vec{s} \rangle$ for a nucleus always follows the field smoothly or "adiabatically." However, when the variation of $\vec{h}_A$ is very large, we expect some abrupt readjustments of the neighboring spins to occur since the applied field influences every spin directly. Such abrupt readjustments of the neighborhood cause random changes on the local fields and interrupts the adiabatic change. In short, turning $\vec{h}_A$ on or off effectively stirs up the spins and causes readjustments. The probability for adiabatic change to survive when the applied field is changed by h_A is expected to follow

$$P(h_A) = e^{-h_A/h_M} , \tag{6.1}$$

where h_M can be estimated roughly as follows.

When the applied field is changed by the amount h_A, it affects each spin energy by $\sim h_A$. Assuming that the spins in the neighborhood of the nucleus are randomly oriented, we expect the change of energy in the neighborhood to be roughly $\sqrt{n}\,h_A$ plus the change in exchange energy, where n is some effective number of neighbors. We argued earlier [see following Eq. (3.3)] that $n \sim 10$. This change of energy is an estimate of the change of the barrier height for the metastable state. When it is comparable to the barrier height itself, the metastable state may become unstable and decays right away, or decays faster due to a decrease in barrier height. The barrier height could increase as a result, too. However, the probability for this is small. The energy most likely would increase (and hence the barrier height decreases) as a result of stirring, not decrease. We can also look at the effect still another way. Since $\vec{h}_A$ directly affects all the spins, it does not have to be large to produce an abrupt change of at least one of the spins in the neighborhood. Since a field change of order 1 would most likely produce sizable changes for all spins, we expect h_M to be $\sim 1/n$. These arguments are all very crude, but it is safe to say that h_M should be a fraction of unity.

B. Thermal remanent magnetization (TRM)

We can gain some qualitative understanding by looking at simple sketches of the distribution of $\vec{h}$. The sample is cooled with the field $\vec{h}_A$ on. Thus we expect a distribution centered around $\vec{h}_A$ but with a cavity around $\vec{h}=0$, as shown in Fig. 9(a). This cavity is created to minimize energy as the system is cooled down. Now turn off the field $\vec{h}_A$. If h_A is not too large, the distribution ends up centered around zero with a cavity around $-\vec{h}_A$ with little change in shape. This is shown in Fig. 9(b). The deficiency of spins pointing in $-\vec{h}_A$ direction due to the cavity thus produces a total net spin in $\vec{h}_A$ direction. This gives the remanent magnetization. Clearly the remanent increases with h_A linearly for small h_A. For larger h_A, the increase is diminished by random changes of spins mentioned above. The remanent thus is expected to decrease for large h_A.

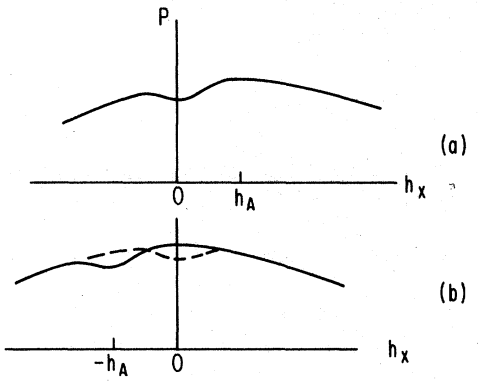

FIG. 9. TRM: (a) Distribution of h_x before h_A is turned off ($\vec{h}_A$ along x direction) and (b) shortly after h_A is turned off.

The decay of metastable states then gradually moves the cavity to the center and the remanent magnetization thus decays. Based on this qualitative picture of TRM, we can easily write down an expression for the remanent magnetization $\vec{m}$ per nucleus plus neighbors

$$\vec{m}=\left[\int d\Lambda\rho(\Lambda)e^{-\gamma t}\right]\int d^3h\bar{P}_0(\vec{h})\langle\vec{S}\rangle C'(\vec{h})p(h_A) \ , \tag{6.2}$$

where $\langle\vec{S}\rangle=\vec{h}/\Lambda+\langle\vec{s}_n\rangle$ is the average total spin (nucleus and neighbors), C' is a cavity factor, and $p(h_A)$ is the decay factor [Eq. (6.1)] due to large h_A. For small h_A, we can expand Eq. (6.2) to first order and use Eq. (5.9) for C' to obtain simply

$$\vec{m}(t)\approx|\chi^*(t)|\vec{h}_A \ , \tag{6.3)}$$

where $\chi^*(t)$ is the time-dependent susceptibility evaluated in Sec. V [see Eqs. (5.6)–(5.11)]. This is of course expected since it is the same cavity shift which produces the magnetization in both cases. For χ^*, the cavity center shifts from 0 to $\vec{h}_A$ as $\vec{h}_A$ is turned on, and back toward zero as metastable states decay. For TRM, the cavity center shifts from 0 to $-\vec{h}_A$ when $\vec{h}_A$ is turned off, and toward zero as metastable states decay.

Equation (6.2) is valid also for larger values of h_A. The dominating dependence of h_A comes from the survival probability $p(h_A)$ given by Eq. (6.1), since h_M is small compared to the scales of h and Λ in the integral. Thus, we simply have

$$\vec{m}_{\rm TRM}(t)\approx|\chi^*(t)|\vec{h}_A e^{-h_A/h_M} \ . \tag{6.4}$$

As a function of h_A, $m(t)$ has a peak at $h_A=h_M$.

C. Isothermal remanent magnetization (IRM)

Again let us gain some qualitative understanding by looking at some sketches of field distributions for the nuclei. In this case, the sample was cooled without external field. So we start with Fig. 10(a), which shows a cavity around $\vec{h}=0$. Now we turn on $\vec{h}_A$. The whole distribution is shifted by $\vec{h}_A$. Then we turn off $\vec{h}_A$, the whole distribution gets shifted back. Therefore if h_A is very small, there is no change at the end, i.e., no remanent magnetization. However, for h_A not small, other things can happen. As we discussed earlier, h_A causes decay. Thus, it would create a cavity around zero and also makes the cavity around $\vec{h}_A$ shallower as shown in Fig. 10(b). The larger h_A, the stronger the effect. Now we turn off $\vec{h}_A$. The result is a cavity at $-\vec{h}_A$ [see Fig. 10(c)], as well as one at the origin. We therefore have a nonvanishing remanent. The cavity generated at the origin of Fig. 10(b) is expected to have an amplitude proportional to $1-e^{-h_A/h_M}$. It will diminish by a factor e^{-h_A/h_M} when it is shifted to $-\vec{h}_A$ in Fig. 10(c). One immediately arrives at the reasonable conclusion that the remanent can be fitted by

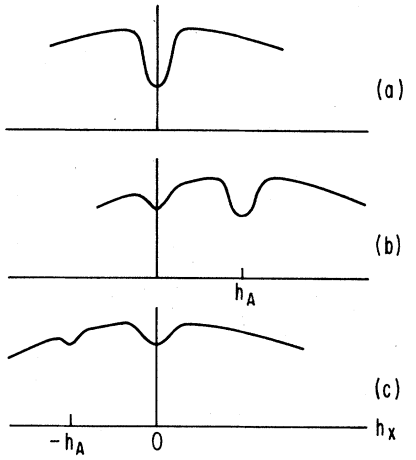

FIG. 10. IRM: (a) Initial distribution; (b) turn on h_A; (c) h_A turned off. The cavities are exaggerated for the clarity of illustration.

$$\vec{m}_{\rm IRM}(t)\approx|\chi^*(t)|\vec{h}_A(1-e^{-h_A/h_M})e^{-h_A/h_M} \ . \tag{6.5}$$

This should be good for $\vec{h}_A$ not too small. It essentially assumes that changing the field by a large amount has the same effect as that of heating up the system as far as stirring up the spins goes. After the stirring stops the spins settle down very much like they settle down when the temperature is decreased. Therefore, for very large h_A, the cavity created around $\vec{h}=0$ in Fig. 10(b) should be comparable in size and shape as that in Fig. 9(a), which was a result of cooling down from a higher temperature.

D. Saturation remanent

Experimental results indicate that both TRM and IRM approach an asymptotic "saturation remanent magnetization" for large h_A. Our results [Eqs. (6.4) and (6.5)] show that IRM and TRM vanish for large h_A, and fail to account for the saturation remanent. This is not surprising in view of the crudeness of our approximations. Our argument for the factor $\exp(-h_A/h_M)$ of Eq. (6.1) was that h_A stirs up the spins and the average spin thus vanishes for large h_A. This conclusion is accurate within an error of $O(1\sqrt{n})$ where n is the number of neighbors. Thus, a saturation remanent of the order

$$m_s\sim|\chi^*|h_M/\sqrt{n} \tag{6.6}$$

is consistent with our arguments.

Figure 3 summarizes our conclusions on the remanent magnetizations.

VII. DISCUSSION

A. Comparison with other models

As a result of the vector nature of spins, the spin configurations in this vector model are "soft" as opposed to the rigid configurations in the Ising spin-glass model. We have constructed nuclei by putting together strongly coupled pairs, trios, or more spins. A metastable state is a result of cooperative behavior of a nucleus and its neighbors. In contrast, the metastable state in Ref. 5 for the Ising model involves only the nucleus. The neighbors are rigid.

The anisotropy energy tensor for a nucleus is also a consequence of the vector nature of spins. The barrier height of a metastable state is of the order h^{*2}/J which is smaller for larger J. For the Ising model, the barrier height is larger for larger J.

The quantum nature of this vector model allows a simple calculation of the anisotropy energy tensor, which would be more difficult to obtain in a purely classical vector model such as that in Ref. 7.

The r^{-3} interaction and the dimension three are special for our calculation above, although the basic theory of Sec. II is quite general. For short range, Gaussian-distributed interactions, there would be far fewer nuclei, for example.

The cluster picture is quite common in various branches of many-body physics. One usually tries to stress the similarities of different cluster approaches. The more recent theory of glasses by Anderson, Halperin, and Varma[10] approximated the low-lying states by those of a set of two-level systems. The linear temperature dependence of the specific heat, among other observed results, followed. As was pointed out in Ref. 5, the clusters in the Ising spin-glass resembled the two-level system, of Anderson *et al.* Again here we have nuclei which resemble these two-level systems. However, there are some important differences, too. For example, the specific heat in Ref. 5 came from single-spin excitations, not the metastable two-level systems, and in Ref. 7 the specific heat came mainly from collective modes, i.e., the spin waves, not any cluster. The cluster in Ref. 5, and the nuclei here, play an important role in metastability, i.e., in dynamics, not in specific heat. The two-level systems of Ref. 10 were proposed to characterize the basic energy-level structure of glasses, not so much the metastability.

We have emphasized the change of neighboring spins of a nucleus when the spin of the nucleus is changed. Such change is very important in the formation of metastable states (see Sec. II C). This change is parallel to the role of "reaction field" as discussed by Cyrot.[11] The discussion of Sec. III in the correction to local-field distribution can be in some sense indirectly related to the idea of the reaction field.

We note that the concept of "anisotropy" has been extensively used in analyzing experimental data on spin-glass (see for example Ref. 1 and reference cited therein, Ref. 12). There has been some theoretical effort to find a justification (e.g., Ref. 11). The notion of anisotropy fields and tensors introduced in Sec. II seem to serve as a simple and natural justification directly following the mean-field approximation.

It should be emphasized that this anisotropy concept discussed above is a local anisotropy seen by nuclei. It is not the anisotropy involved in the electron spin resonance (ESR) line-shift and -broadening experiments, which comes from spin nonconserving interactions such as spin-orbit, dipolar, and crystal fields. These nonconserving interactions are not included in our model. They have to be included in order to calculate ESR observed quantities. Recently there have been ESR experiments[13] and phenomenological theory.[14]

B. Quantitative calculation

The picture provided by the mean-field approximation formulated above is that of a set of single spins and nuclei, each in self-consistent fields $\vec{h}$ and $K^*_{\mu\nu}$. This is essentially a semiclassical approximation. Quantum mechanics enters only in determining the structure of nuclei and $K^*_{\mu\nu}$. This picture points to the direction of a more quantitative calculation. With the structure of nuclei and $K^*_{\mu\nu}$ ready, one can sample the statistics of spins, nuclei, and local fields by numerical simulation. The simulation program will be similar to those in Refs. 5 and 7 but will be more involved.

The qualitative picture of the cavity in the field distribution and the concept of h_M, the memory field, should remain useful in a quantitative analysis.

C. Comparison with experiments

The above rough calculation is mainly a preliminary check on the ideas formulated in Sec. II. Although exhaustive comparison with the vast amount of data available is not warranted at this stage, we see that our crude results above do describe qualitatively some of the observations.

The main result here is the estimate for the time dependence of the susceptibility and the remanent magnetization. This time dependence is summarized in Fig. 2 for χ^* vs $T\ln(t/\tau)$. In our crude approximation, the remanent magnetization is proportional to $|\chi^*|$. Its plot versus $T\ln(t/\tau)$ would just be Fig. 2

upside down since χ^* is negative. For $T \ll T_c$ ($T_c \sim 1$ in our units), the plot of χ^* vs $\ln t$ over one or two decades of t would be just a segment of the curve in Fig. 2 and would thus appear as a straight line. Experimental data are often fitted to a small exponent aT defined by

$$|\chi^*| \propto t^{-aT} , \quad a = \frac{d}{dx} \ln|\chi^*| , \tag{7.1}$$

where $x \equiv T \ln(t/\tau)$ is the absissa of Fig. 2. It is clear that the value of a depends on which segment of the curve in Fig. 2 is plotted. It depends on the value of $T \ln(1/\tau)$ crucially for a given range of t, which is often 1−1000 seconds. Although the definition of τ is far from precise, the values of τ vary considerably among different spin-glasses. For example, for $(LaGd)Al_2$, Löhneysen and Tholence[3] gave $\tau \sim 10^{-6}$ sec; for MnCu, the estimate of Prejean[1] would imply $\tau \sim 10^{-13}$ sec.

According to Fig. 2, we have $a \approx 0$ for very small $x = T \ln(1/\tau)$. For $x \gtrsim 1$, $|\chi^*|$ roughly decays exponentially in x and $a \approx 0.3$. Since $T_c \sim 1$ in our units, a^{-1} is roughly a few times larger than T_c. These results are in qualitative agreement with observations. (Note that aT can be identified as α of Ref. 3, and a^{-1} is T_0 of Prejean, Ref. 1.)

The above results show also that, for $T \ll T_c$, the susceptibility is an increasing function of T. The magnitude of χ at $T = 0$ is smaller by a factor of 4 or 5 than that at T_c (estimated by Curie law), according to our analysis. Because of the uncertainties in the number of nuclei, the parameter T_m, and the effective number of neighbors per nucleus, the estimate of the magnitude of χ is very crude. These uncertainties do not enter in the analysis of the time variation discussed above.

The observed falling off of the remanent magnetization as a function of the applied field[1,3] is explained in Sec. VI as a consequence of the decay of spin memory due to the stirring effect of varying the applied field.

We can apply our analysis above to examine the hysteresis loop. We would get a simple smooth loop. Recent experiments[12] on hysteresis show that some spin-glasses show smooth loops, but some exhibit sudden reversals of a large fraction of spins. Such sudden reversals were attributed to effects of spin-orbit interactions. Clearly, much more theoretical work is needed.

ACKNOWLEDGMENT

It is a pleasure to thank Professor Sheldon Schultz for numerous stimulating conversations and for providing experimental information. The author is also indebted to Dr. Philippe Monod, Dr. Chandan Dasgupta, and Professor Amnon Aharony for helpful discussions and references. He is also grateful to Dr. Dasgupta and Professor Wayne Saslow for carefully reading and commenting on the manuscript. This work is supported in part by the National Science Foundation under Grant No. DMR-77-04679.

APPENDIX

1. Derivation of the local-field distribution assuming random positions and orientations of spins

First we express the distribution as a Fourier integral

$$P(\vec{h}) = \left\langle \delta\left[\vec{h} - \tfrac{1}{2}\sum_j J_{ij}\hat{h}_j\right]\right\rangle$$
$$= \int d^3\xi (2\pi)^{-3} e^{i\vec{\xi}\cdot\vec{h}} \prod_j \langle e^{-i\vec{\xi}\cdot\hat{h}_i J_{ij}/2}\rangle . \tag{A1}$$

Each average is over $J_{ij} = \pm 4/r^3$ and orientations $\hat{h}_j$:

$$C(\xi) \equiv \langle e^{-i\vec{\xi}\cdot\hat{h}_j J_{ij}/2}\rangle$$
$$= \frac{1}{V}\int_{V_0}^{V} dv \frac{1}{4\pi}\int d\hat{h} e^{-2i\vec{\xi}\cdot\hat{h}/r^3} , \tag{A2}$$

where $dv \equiv 4\pi r^2 dr$ and V is a spherical volume centered at $r = 0$. We have introduced a lower cutoff $V_0 \equiv \frac{4}{3}\pi r_0^3$ to exclude the possibility of spins closer to the origin than some minimum distance r_0. We shall make use of this cutoff later.

The integral over the solid angles $d\hat{h}$ is easily done. In the limit of large V, we have

$$C(\xi) = 1 + \frac{1}{V}\int_{V_0}^{\infty} dv \left(\frac{r^3}{2\xi}\sin\frac{2\xi}{r^3} - 1\right)$$
$$= 1 - \frac{8\pi}{3h_0}\frac{g(h_0\xi)}{V} , \tag{A3}$$

where the function g is defined by

$$g(x) \equiv x\int_0^x \frac{dy}{y^2}\left(1 - \frac{1}{y}\sin y\right)$$
$$= -\sum_{n=1}^{\infty} \frac{(-x^2)^n}{(2n-1)(2n+1)!}$$
$$= \tfrac{1}{4}\pi x - 1 + x\int_x^{\infty} \frac{dz}{z^3}\sin z \tag{A4}$$

and

$$h_0 \equiv 2/r_0^3 .$$

Let there be N spins in the volume V. In the large V

limit, we have from Eq. (A3)

$$C(\xi)^N = \exp\left[-\frac{8\pi}{3h_0} g(h_0\xi)\frac{N}{V}\right] . \tag{A5}$$

In our units, $N/V = 1$. Substituting Eq. (A5) in Eq. (A1), we obtain

$$P(\vec{h}) = \int d^3\xi (2\pi)^{-3} \exp[i\vec{\xi}\cdot\vec{h} - (8\pi/3h_0) g(h_0\xi)] . \tag{A6}$$

In the limit of $h_0 \to \infty$, we have $(8\pi/3h_0)g(h_0\xi) \to \frac{2}{3}\pi^2\xi$. The ξ integral is then easily evaluated to give

$$P(\vec{h}) = \tfrac{2}{3}[(\tfrac{2}{3}\pi^2)^2 + h^2]^{-2} . \tag{A7}$$

For finite h_0, we can evaluate $P(\vec{h})$ approximately using the first term of the series in Eq. (A4):

$$\frac{8\pi}{3h_0} g(h_0\xi) \approx \tfrac{1}{2}(\tfrac{8}{9}\pi h_0)\xi^2 \tag{A8}$$

to obtain

$$P(\vec{h}) \approx (2\pi\mu_0^2)^{-3/2} e^{-h^2/2\mu_0^2} , \quad \mu_0^2 \equiv \tfrac{8}{9}\pi h_0 . \tag{A9}$$

This form is of course what the central limit theorem would imply. It makes sense only if we integrate it over a range comparable to μ_0.

2. Joint distribution $P(\vec{h}, \vec{h}^*)$

Using the same method and under the same assumptions as above, we can calculate the distribution function for $\vec{h} = \frac{1}{2}(\vec{h}_1 + \vec{h}_2)$ and $\vec{h}^* = \frac{1}{2}(\vec{h}_1 - \vec{h}_2)$ for a pair $\vec{s}_1, \vec{s}_2$. Write

$$P(\vec{h}, \vec{h}^*) = \langle \delta(\vec{h} - \tfrac{1}{2}(\vec{h}_1 + \vec{h}_2))\delta(\vec{h}^* - \tfrac{1}{2}(\vec{h}_1 - \vec{h}_2))\rangle , \tag{A10}$$

$$\tfrac{1}{2}(\vec{h}_1 \pm \vec{h}_2) = \tfrac{1}{2}\sum_j (J_{1j} \pm J_{2j})\frac{\hat{h}_j}{2} = \sum_j \left(\frac{\tau_{1j}}{r_{1j}^3} \pm \frac{\tau_{2j}}{r_{2j}^3}\right)\hat{h}_j . \tag{A11}$$

Similar to Eq. (A1), we obtain

$$P(\vec{h}, \vec{h}^*) = (2\pi)^{-6} \int d^3\xi d^3\xi^* \exp(i\vec{\xi}\cdot\vec{h} + i\vec{\xi}^*\cdot\vec{h}^*) \times C(\vec{\xi}, \vec{\xi}^*)^N , \tag{A12}$$

$$C(\vec{\xi}, \vec{\xi}^*) = \left\langle \exp\left[-i\vec{\xi}\cdot\hat{h}\left(\frac{\tau_1}{r_1^3} + \frac{\tau_2}{r_2^3}\right) - i\vec{\xi}^*\cdot\hat{h}\left(\frac{\tau_1}{r_1^3} - \frac{\tau_2}{r_2^3}\right)\right]\right\rangle .$$

We shall make the approximation $r_1 \approx r_2$; i.e., we assume that the distance between spins 1,2 is small compared to their distances to spin j, or, $J_{12} >> J_{1j}, J_{2j}$. Since $|\tau_1 \pm \tau_2|$ is either two or zero, Eq. (A12) becomes simply

$$C(\xi, \xi^*) = \tfrac{1}{2}[\langle e^{-2i\vec{\xi}\cdot\hat{h}/r^3}\rangle + \langle e^{-2i\vec{\xi}^*\cdot\hat{h}/r^3}\rangle] = \tfrac{1}{2}[C(\xi) + C(\xi^*)] , \tag{A13}$$

where $C(\xi)$ is given by Eq. (A2), and hence Eq. (A3). It follows that $\vec{h}$ and $\vec{h}^*$ are independent, and

$$P(\vec{h}, \vec{h}^*) = \bar{P}_0(\vec{h})\bar{P}_0(\vec{h}^*) , \tag{A14}$$

$$\bar{P}_0(\vec{h}) \equiv \int d^3\xi (2\pi)^{-3} \exp[i\vec{\xi}\cdot\vec{h} - (4\pi/3h_0) g(h_0\xi)] ,$$

which differs from Eq. (A6) only in an extra factor $\frac{1}{2}$ in front of $g(h_0\xi)$.

For small h, we have

$$\bar{P}_0(\vec{h}) = \tfrac{1}{3}[(\tfrac{1}{3}\pi^2)^2 + h^2]^{-2}$$

and for large h, we have

$$\bar{P}_0(\vec{h}) = (\pi\mu_0^2)^{-3/2} e^{-h^2/\mu_0^2} , \tag{A15}$$

where μ_0^2 is given by Eq. (A9).

3. Derivation of the effective Hamiltonian for the strongly coupled spin trio

We write the Hamiltonian H_{123} in two parts:

$$H_{123} = H_0 + \mathcal{H} , \tag{A16}$$

$$H_0 = -J_{12}\vec{s}_1\cdot\vec{s}_2 - J_{23}\vec{s}_2\cdot\vec{s}_3 - J_{31}\vec{s}_3\cdot\vec{s}_1$$

and $\mathcal{H}$ is the rest of H_{123} as given in Eq. (2.25). We assume J_{12} is the largest of the three J's. Without losing much generality, we simplify the algebra greatly by assuming $J_{23} = J_{31} \equiv J$. We have, writing K for J_{12}

$$H_0 = -K\vec{s}_1\cdot\vec{s}_2 - J(\vec{s}_1 + \vec{s}_2)\cdot\vec{s}_3 . \tag{A17}$$

The energies are now very easy to find. We obtain a quartet and two doublets:

$$E_0^{(0)} = -\tfrac{1}{4}K - \tfrac{1}{2}J ,$$
$$E_1^{(0)} = -\tfrac{1}{4}K + J , \tag{A18}$$
$$E_2^{(0)} = \tfrac{3}{4}K .$$

Now we can use the standard second-order perturbation theory to calculate the splitting of the quartet levels. The new quartet levels are eigenvalues of an

operator H_{eff} in the four-dimensional subspace of the quartet

$$H_{\text{eff}} = E_0^{(0)} - \frac{1}{\Delta E} Q\mathcal{H}D_1\mathcal{H}Q - \frac{1}{\Delta E_2} Q\mathcal{H}D_2\mathcal{H}Q \ , \tag{A19}$$

where Q is the projection operator for the quartet subspace, D_1 and D_2 are those for the two doublet subspaces, respectively, and $\Delta E_{1,2} \equiv E_{1,2}^{(0)} - E_0^{(0)}$. Let us write $\mathcal{H}$ as

$$\mathcal{H} = -\vec{h}_1^* \cdot \vec{\mu}_1 - \vec{h}_2^* \cdot \vec{\mu}_2 \ , \ \vec{\mu}_{1,2} \equiv \vec{s}_{1,2} - \vec{s}_3 \ , \tag{A20}$$

then

$$\mathcal{H}D\mathcal{H} = h_{1\alpha}^* h_{1\beta}^* \mu_{1\alpha} D \mu_{1\beta} + h_{2\alpha}^* h_{2\beta}^* \mu_{2\alpha} D \mu_{2\beta} + h_{1\alpha}^* h_{2\beta}^* (\mu_{1\alpha} D \mu_{2\beta} + \mu_{2\beta} D \mu_{1\alpha}) \ , \tag{A21}$$

where repeated α, β imply summation over x,y,z. Each term of Eq. (A21) involves a tensor operator, e.g., $\mu_{1\alpha} D \mu_{1\beta}$. In view of the Wigner-Eckart theorem (or, simply by symmetry), the matrix elements of a tensor operator in the quartet subspace must be proportional to a combination of those of $s_\alpha s_\beta$ and the identity, e.g.,

$$Q \mu_{1\alpha} D \mu_{1\beta} Q = a s_\alpha s_\beta + b \delta_{\alpha\beta} \ , \tag{A22}$$

where a,b are constants. To determine a,b, we simply set $\alpha = \beta = z$ and calculate two matrix elements of both sides, and then solve for a and b. In particular, take $|\frac{3}{2}\rangle$ and $|\frac{1}{2}\rangle$, i.e., $s_z = \frac{3}{2}$ and $\frac{1}{2}$, we obtain for D_1:

$$\begin{aligned} &0 = a(\tfrac{3}{2})^2 + b \ , \\ &\langle \tfrac{1}{2} | \mu_{1z} D_1 \mu_{1z} | \tfrac{1}{2} \rangle = \tfrac{1}{2} = a(\tfrac{1}{2})^2 + b \ , \\ &a = -\tfrac{1}{4}, \quad b = \tfrac{9}{16} \ . \end{aligned} \tag{A23}$$

This procedure applies to all the other terms in $\mathcal{H}D\mathcal{H}$ of Eq. (A21). The algebra is straightforward. After we express H_{eff} entirely in terms of $\vec{s}$ operators, we obtain the form Eq. (2.26) with

$$A = \frac{1}{6J}\left(1 + \frac{J}{2K+J}\right) \ , \quad B = \frac{1}{6J}\left(1 - \frac{J}{2K+J}\right) \ , \tag{A24}$$

$$E_0 = E_0^{(0)} - \tfrac{9}{4} A (h_1^{*2} + h_2^{*2}) - \tfrac{9}{2} B \vec{h}_1^* \cdot \vec{h}_2^* \ .$$

The anisotropy energy tensor $K_{\mu\nu}^*$ defined by (2.26) and (2.27) is

$$K_{\mu\nu}^* = A(h_{1\mu}^* h_{1\nu}^* + h_{2\mu}^* h_{2\nu}^*) + B(h_{1\mu}^* h_{2\mu}^* + h_{2\mu}^* h_{1\nu}^*) \ . \tag{A25}$$

This tensor is defined by two vectors, $\vec{h}_1^*$ and $\vec{h}_2^*$. Therefore two of its principal axes are in the plane defined by $\vec{h}_1^*$ and $\vec{h}_2^*$. The third is perpendicular to the plane and has zero principal radius.

In the plane, the trace and determinant of K^* are, respectively,

$$\begin{aligned} &TrK^* = A(h_1^{*2} + h_2^{*2}) + 2B\vec{h}_1^* \cdot \vec{h}_2^* \ , \\ &\det K^* = (A^2 - B^2)(\vec{h}_1^* \times \vec{h}_2^*)^2 \ . \end{aligned} \tag{A26}$$

From Eq. (A26), the two nonzero eigenvalues of K^* are readily obtained. They are both nonzero provided that $\vec{h}_1^*$, $\vec{h}_2^*$ are not collinear. The two lowest-energy configurations have $\vec{s}$ pointing perpendicular to $\vec{h}_1^*$ and $\vec{h}_2^*$.

[1] J. J. Prejean, J. Phys. (Paris) Colloq. 39, C6-970 (1978); A. Blandin, *ibid.* 39, C6-1499 (1978).

[2] S. Nagata, P. H. Keesom, and R. H. Harrison, Phys. Rev. B 19, 1633 (1979); D. L. Martin, *ibid.* 20, 368 (1979).

[3] H. v. Löhneysen and J. L. Tholence, Phys. Rev. B 19, 5858 (1979).

[4] W. Kinzel, Phys. Rev. B 19, 4595 (1979); D. Stauffer and K. Binder, Z. Phys. B 30, 331 (1978).

[5] C. Dasgupta, S. Ma, and C. H. Hu, Phys. Rev. B 20, 3837 (1979).

[6] See for example, D. Mattis, *The Theory of Magnetism* (Harper and Row, New York, 1965), p. 197.

[7] L. R. Walker and R. E. Walstedt, Phys. Rev. Lett. 38, 514 (1977).

[8] W. Y. Ching, K. M. Leung, and D. L. Huber, Phys. Rev. Lett. 39, 729 (1977); R. G. Palmer and C. M. Pond (unpublished).

[9] F. W. Smith, Phys. Rev. B 14, 241 (1976).

[10] P. W. Anderson, B. I. Halperin, and C. M. Varma, Philos. Mag. 25, 1 (1972).

[11] M. Cyrot, Phys. Rev. Lett. 43, 173 (1979).

[12] P. Monod, J. J. Prejean, and B. Tissier, J. Appl. Phys. 50, 7324 (1979); J. J. Prejean, N. J. Joliclerc, and P. Monod (unpublished).

[13] P. Monod and Y. Berithier (unpublished).

[14] W. M. Saslow, Phys. Rev. B (in press).